# Periodic and Metallic Nano-structures Patterned by Contact Transfer Lithography with Application on Localized Surface Plasmon Resonance

Hao-Yuan Chung, Chun-Ying Wu and Yung-Chun Lee
*Department of Mechanical Engineering, National Cheng-Kung University, Tainan, Taiwan*

Keywords: Localized Surface Plasma Resonance, Metallic Nano-structures, Contact Transfer Lithography.

Abstract: In this study, we demonstrate a rapidly, low cost, and mass production process to fabricate arrayed metallic nanoparticles on a variety of substrates based on contact transfer and metal mask embedded lithography (CMEL). A hexagonal arrayed metallic nanoparticles deployed on ITO/glass substrate with sub-micron periodicity is achieved. It is observed in optical transmittance measurements that noble metallic arrayed nanoparticles deployed on ITO/glass substrate result in a spectrally narrowband of extinction in visible range, and is in good agreement with the simulated results using finite-element method (FEM). It is found that the narrowband extinction spectrum is associated with electromagnetic field coupling between the arrayed metallic nanostructures and the ITO layer. This electromagnetic field coupling induces significant plasmon resonance in the ITO layer underneath the arrayed metallic nanostructures. Based on this observed phenomenon and our innovative large-area nano-fabrication processes, optoelectronic devices with arrayed metallic nanostructures can be easily designed and developed.

## 1 INTRODUCTION

Arrayed metallic nanoparticles have gained lots of attentions in both scientific researches as well as engineering application during last few decades. Metallic nanostructures exhibit a rich variety of intriguing optical properties due to the interaction of the electromagnetic field with the free electrons of the metal. Such an excitation can occur at a metal-dielectric interface and is called surface-plasmon polariton or at a metallic nanoparticle, and in this case it is termed as particle-plasmon polariton (Linden, Kuhl, and Giessen, 2001; Hutter and Fendler, 2004; Yannopapas and Stefanou, 2004)

There are several ways to achieve metallic nanoparticles, such as laser ablation method, chemical reduction method and pyrolysis method (Mafune et al., 2001; Pillai et al., 2007). These methods can produce nanoparticles over large area but have limitations to efficiently deploy nanoparticles in specified arrangements. Electron beam lithography is an excellent method to fabricate arrayed metallic nanoparticles. The size of nanoparticle can be well controlled to about several tens of nanometers and arranged into square or triangular lattice (Linden, Kuhl, and Giessen, 2001). However, the costs of equipment and time-consuming issues limit the capability to mass produce large-area devices.

In this study, we demonstrate a rapidly, low cost, and mass productive process to deploy arrayed metallic nanoparticles on a variety of substrates based on contact-transfer and mask-embedded lithography (CMEL). A hexagonal arrayed metallic nanoparticles deployed on an ITO/glass substrate with sub-micron periodicity is obtained. Moreover, the optical transmittance spectrum of the sample is measured via spectrophotometer experimentally and a numerical simulation using finite-element method (FEM) is carried out to identify the mechanisms of observed resonance characteristics.

## 2 EXPERIMENTAL DETAILS AND RESULTS

This section describes the experimental details to fabricate arrayed metallic nanoparticles on a variety of substrates. A nanoimprinting process presented in our previous study (Lee and Chiu, 2008), CMEL, is applied to define and pattern arrayed metallic structures which have feature sizes in sub-micron or nanometer scales. First of all, a hexagonal arrayed


Chung H., Wu C. and Lee Y..
Periodic and Metallic Nano-structures Patterned by Contact Transfer Lithography with Application on Localized Surface Plasmon Resonance.
DOI: 10.5220/0005333500200025
In *Proceedings of the 3rd International Conference on Photonics, Optics and Laser Technology* (PHOTOPTICS-2015), pages 20-25
ISBN: 978-989-758-092-5

structured silicon mold is prepared using electron beam lithography. The diameter of each holed structure is 200 nm and the periodicity of hexagonal array is 400 nm. A flexible h-PDMS mold replicated from the silicon mold is then obtained to act as the imprinting mold used in CMEL process. This h-PDMS mold is inexpensive compared to the primary silicon mold thus could be disposable after being contaminated or damaged during the imprinting process. Furthermore, this flexible mold has benefit to minimize the contact issue in imprinting process and utilize large-area pattern transfer successfully. Figure 1 illustrates the procedures to fabricate arrayed metallic nanostructures. An h-PDMS concave mold deposited with gold film is contacted to the top surface of polymer film coated on substrate and then heating to the glass transition temperature (Tg) of the polymer film. After cooling down to room temperature, the patterned gold film is transferred from the h-PDMS mold to the polymer film owing to the good adhesion between metal-polymer interfaces. This patterned gold film is then acted as etching mask in dry etching process to obtain a patterned polymer nanostructure. Combining with lift-off and thermal annealing processes, it is possible to fabricate arrayed metallic nano-disks and nanoparticles on a variety of substrates.

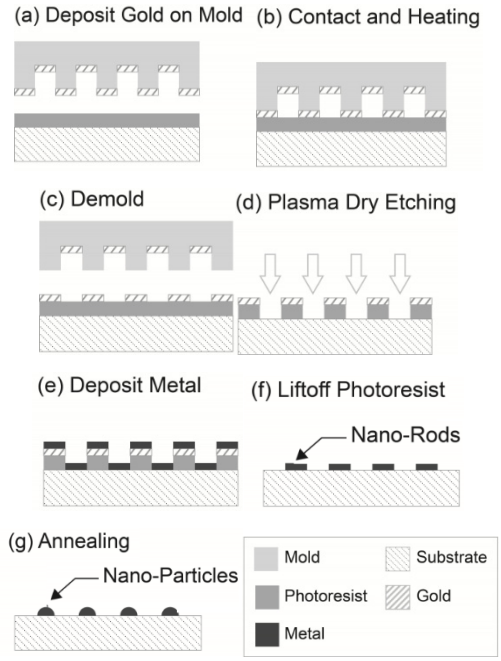


Figure 1: The procedure of using: (a-d) CMEL process, (e-f) lift-off, and (g) thermal annealing processes, to achieve an arrayed metallic nanoparticle.

Figure 2 shows the SEM image of the hexagonal arrayed Au nano-disks (AuNRs) deployed on a 230 nm thick ITO film deposited on a soda-lime glass substrate. The periodicity of hexagonal array is 400 nm; the dimensions of AuNRs are 200 nm in diameter and 40 nm in thickness. The overall size of arrayed metallic nanostructures is about 1 $cm^2$.

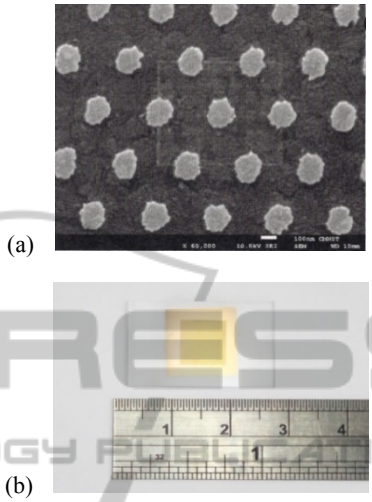


Figure 2: (a) SEM images of the hexagonal arrayed AuNRs deployed on 230 nm thick ITO film on top of a glass substrate. The periodicity of hexagonal array is 400 nm; the dimensions of AuNRs are 200 nm in diameter and 40 nm in thickness. (b) The overall size of arrayed AuNRs is about 1 $cm^2$.

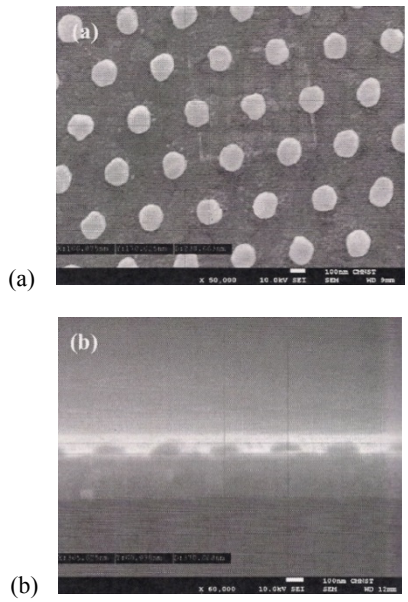


Figure 3: SEM images of (a) the top view and (b) the side view of hexagonal arrayed AuNPs deployed on a 230 nm thick ITO film on top of a glass substrate. Periodicity of hexagonal array is 400 nm; the radius of AuNPs is 85 nm.

Figure 3 shows the SEM images of the hexagonal arrayed Au nanoparticles (AuNPs) deployed on an ITO/glass substrate. During rapidly thermal annealing process, the disk-liked AuNRs were transformed into hemispherical AuNPs. The periodicity of hexagonal array is 400 nm and the radius of AuNPs is 85 nm. According to the experimental results, arrayed metallic nanoparticles deployed on ITO/glass substrates can be achieved. The dimensions, shapes, and arrangements of these arrayed metallic nanostructures can be easily adjusted by using different type of imprinting molds. The size and material combination of the obtained metal particles can be controlled by the thicknesses and varieties of metallic films deposited during the lift-off process.

## 3 OPTICAL MEASUREMENTS AND SIMULATIONS

The optical transmittance spectrum measurement of these arrayed metallic nanoparticles is obtained using a Hitachi U-3010 spectrophotometer. An unpolarized light with wavelength $\lambda_0$ ranging from 400 nm to 1000 nm is normally incident onto the metal side of these samples and the transmitted power is collected at the substrate side. Figure 4 shows the transmittance spectrum of arrayed AuNRs deployed on a glass substrate and on a 230 nm thick ITO film coated on a glass substrate. It is observed that the transmittance spectrum of both samples exhibits a spectrally wideband extinction in near-IR range due to localized surface plasmon resonance. Moreover, significant narrowband extinction in visible range is observed in case of arrayed AuNRs deployed on ITO/glass which means a strong electromagnetic field coupling between the arrayed metallic nanostructures and the ITO layer.

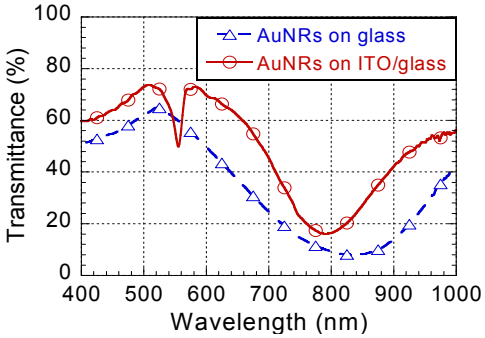


Figure 4: The normal incidence transmittance spectrum measurements of hexagonal arrayed Au nanorods on glass substrate (dashed line) and on a 230 nm thick ITO film on top of a glass substrate (solid line).

A numerical simulation using finite-element method is carried out to identify the resonance phenomenon. Both the transmittance spectrum and the electromagnetic field distribution are obtained to clarify the different mechanisms of resonances in visible and near-IR spectrum. The dielectric functions of Au and ITO are described as Drude model (Rakic et al., 1998; Bender et al., 1998). The dielectric constants of air and glass substrate are $\varepsilon_{air} = 1$ and $\varepsilon_{glass} = 2.31$, respectively.

Figure 5(a) and 5(b) demonstrate the comparisons between the calculated transmittance spectrums and experimental results of arrayed AuNRs and AuNPs on a 230 nm thick ITO film on top of a glass substrate. Figure 6(a) and 6(b) show the simulated and experimental transmittance spectrum of arrayed AgNRs and AgNPs on a 230 nm thick ITO film deposited on a glass substrate, respectively. It is shown that the simulated results are in good agreement with the experimental results. The arrayed metallic nanoparticles deployed on ITO/glass substrate result in a spectrally narrowband extinction in visible and a wideband extinction in near-IR both in experiments and in simulations.

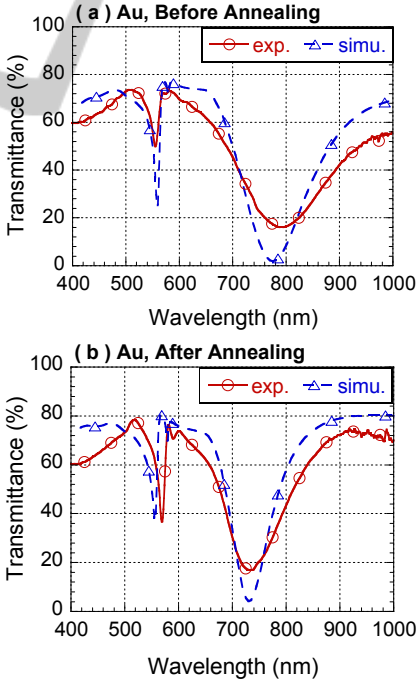


Figure 5: The normal incidence transmittance spectrum measurements (solid line) and the simulated results (dashed line) using FEM. (a) Before annealing, and (b) after annealing.

Figure 7(a) and 7(b) reveal the simulated electromagnetic field distribution of arrayed AuNRs

on a 230 nm thick ITO film deposited on a glass substrate. While the incident wavelength $\lambda_0$ = 775 nm, as shown in Fig. 7, an enhanced electric field around the metallic nano-disks due to localized surface plasmon resonance is observed. Furthermore, Fig. 8(a) and 8(b) show the significant guided mode resonance in the ITO layer underneath the arrayed metallic nanostructures when $\lambda_0$ = 556 nm.

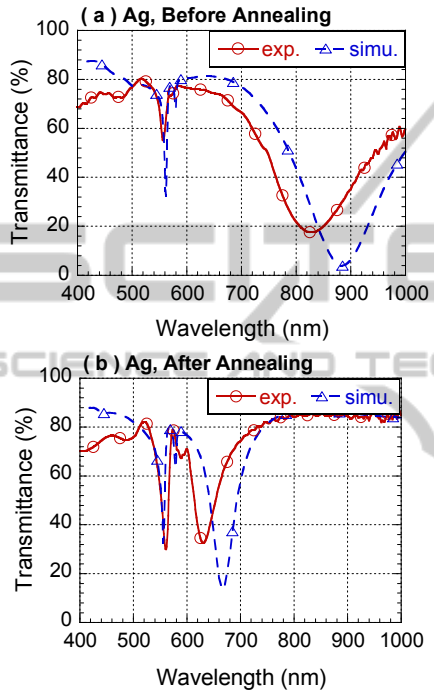


Figure 6: The normal incidence transmittance spectrum measurements (solid line) and the simulated results (dashed line) using FEM. (a) Before annealing, and (b) after annealing.

Figure 7(a) and 7(b) reveal the simulated electromagnetic field distribution of arrayed AuNRs on a 230 nm thick ITO film deposited on a glass substrate. While the incident wavelength $\lambda_0$ = 775 nm, as shown in Fig. 7, an enhanced electric field around the metallic nano-disks due to localized surface plasmon resonance is observed. Furthermore, Fig. 8(a) and 8(b) show the significant guided mode resonance in the ITO layer underneath the arrayed metallic nanostructures when $\lambda_0$ = 556 nm.

A more detail discussion about the guided mode resonance is started from a simple empty-lattice approximation (Christ et al., 2004). As a first step of this approximation, the energy dispersions of the lowest transverse electric (TE0) and transverse magnetic (TM0) guided modes of a homogeneous ITO layer could be found from the solution of the transcendent equations for the asymmetric waveguide slab (Barnoski, 1973, pp. 53-72). It is shown that the calculated dispersions of TE0 and TM0 guided mode of a 230 nm thick ITO slab on thetop of a soda-lime glass substrate. When assuming a surface corrugation with periodicity d of hexagonal array in a second step (in this case, d = 400 nm), the propagation constant is normalized to the reciprocal lattice of the 2D photonic crystal slab which equals to $4\pi/d\sqrt{3}$ . While the propagation constants of $TE_0$ and $TM_0$ equal to the reciprocal lattice, it is shown that the photon energy of TE0 guided modes equal to 2.128 eV. These calculated photon energy of $TE_0$ guided modes are in good agreement with the simulated results using FEM. The shifts of central wavelength might be caused by the neglecting of material and geometry of metallic deployed on the homogeneous ITO waveguide slab.

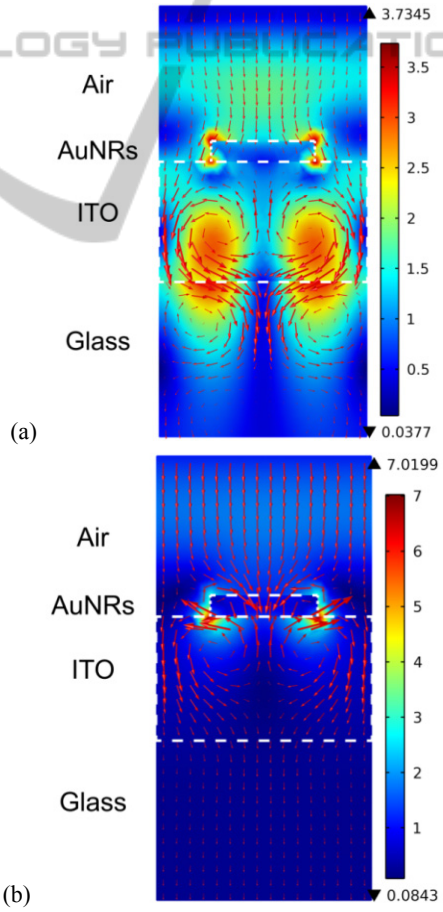


Figure 7: The electromagnetic field distribution of arrayed AuNRs (before annealing) deployed on ITO layer; (a) incident wavelength is 559 nm, and (b) incident wavelength is 775 nm.

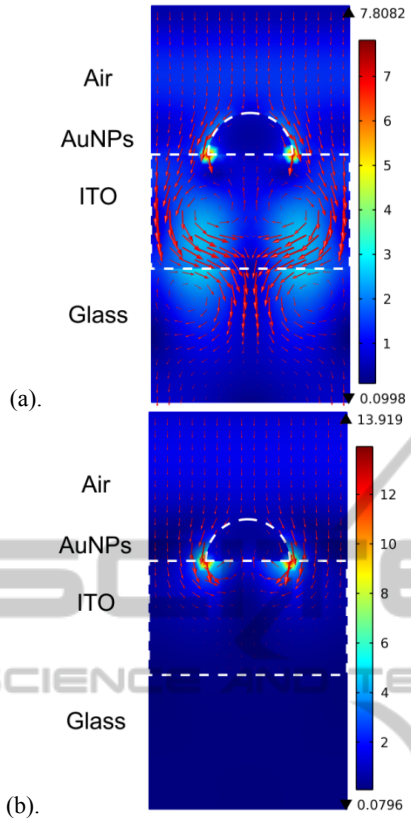


Figure 8: The electromagnetic field distribution of arrayed AuNPs (after annealing) deployed on ITO layer; (a) incident wavelength $\lambda_0$= 556 nm, and (b) incident wavelength $\lambda_0$ = 730 nm.

According to the FEM simulation and empty-lattice approximation discussed above, it suggests that the spectrally narrowband in visible range owing to the guided mode resonance has quite different resonance mechanism with respect to the wideband extinction in near-IR range due to the localized surface plasmon resonance. When an electromagnetic wave normally incident onto arrayed metallic nanostructures, a Bragg's diffraction phenomenon occurs and then couples the electromagnetic wave into the waveguide slab. At certain photon energies of the propagating guided waves which the propagation constant equal to the reciprocal lattice of arrayed nanostructures, a guided mode resonance happens and enhanced electric field distributes within waveguide slab can be observed.

## 4 CONCLUSIONS

In this study, we demonstrate a rapidly, low-cost, large-area, and mass productive fabrication process to obtain arrayed metallic nanostructures on a variety of substrates. The key element in this fabrication method is to combine an innovative metal contact printing lithography with conventional lifting-off and thermal annealing processes. Hexagonal arrays of metallic nanoparticles with sub-micron periodicity are successfully deployed on an ITO/glass substrate. The dimensions, shapes, and arrangements of these arrayed metallic nanostructures and nanoparticles can be easily adjusted by using different pattern designs in the imprinting molds. The sizes and material compositions of the obtained metal nanoparticles can be easily controlled by the deposition thicknesses and material varieties of films deposited during the sample preparation process.

Optical transmittance measurements show that certain kinds of noble metallic arrayed nanoparticles deployed on an ITO/glass substrate can result in a phenomenal narrowband of extinction in spectral range of visible light. Theoretical analysis indicates this narrowband extinction spectrum is associated with electromagnetic field coupling between the arrayed metallic nanostructures and the underlying ITO layer. Numerical simulation based on finite element method is carried out to demonstrate the electromagnetic field distributions of the localized surface plasmon resonance of arrayed metallic nanostructures and the excited waveguide modes within the ITO layer. This electromagnetic field coupling induces significant plasmon resonance in the ITO layer underneath the arrayed metallic nanostructures. A further evidence is attained by comparing the measured transmittance spectrum of a similar noble metallic arrayed nanoparticles deployed on a glass substrate. Experimental results show that the narrowband extinction in visible spectrum is vanished since there is no ITO layer to support guided modes resonance. Based on this observed phenomenon and our innovative large-area nano-fabrication processes, optoelectronic devices with arrayed metallic nanostructures can be easily designed and implemented in the future.

## REFERENCES

Bender, M., Seelig, W., Daube, C., Frankenberger, H., Ocker, B. & Stollenwerk, J. 1998 'Dependence of oxygen flow on optical and electrical properties of DC-magnetron sputtered ITO films', *Thin Solid Film*, vol. 326, pp.72-77.

Barnoski, M. K. 1973. *Introduction to Integrated Optics*, Plenum Press, New York.

Christ, A., Zentgraf, T., Kuhl, J., Tikhodeev, S. G., Gippius, N. A. & Giessen, H. 2004 'Optical properties of planar metallic photonic crystal structures: Experiment and theory', *Phys. Rev B*, vol. 70, p. 125113.

Hutter, E., Fendler, J. H. 2004 'Exploitation of localized surface plasmon resonance', *Adv. Mater.*, vol. 16, pp. 1685-1706.

Lee, Y. C. & Chiu, C. Y. 2008 'Micro-/nano-lithography based on the contact transfer of thin film and mask embedded etching', *J. Micromech. Microeng.*, vol. 18, p. 075013.

Linden, S., Kuhl, J., & Giessen H. 2001 'Controlling the interaction between light and gold nanoparticles: Selective suppression of extinction', *Phys. Rev. Lett.*, vol. 86, pp. 4688-4691.

Mafune, F., Kohno, J. Y., Takeda, Y., & Kondow, T. 2001 'Dissociation and aggregation of gold nanoparticles under laser irradiation', *J. Phys. Chem.*, vol. 105, pp. 9050-9056.

Pillai, S., Catchpole, K. R., Trupke, T. & Green, M. A. 2007 'Surface plasmon enhanced silicon solar cells', *J. Appl. Phys.*, vol. 1019, p. 093105.

Rakic, A. D., Djurisic, A. B., Elazar, J. M. & Majewski, M. L. 1998 'Optical properties of metallic films for vertical-cavity optoelectronic devices', *Appl. Opt.*, vol. 37, pp. 5271-5283.

Yannopapas, V., Stefanou, N. 2004 'Optical excitation of coupled waveguide-particle plasmon modes: A theoretical analysis', *Phys. Rev. B*, vol. 69, p. 012408.